ChemSusChem
Chemistry–Sustainability–Energy–Materials

Chemistry Europe
European Chemical Societies Publishing

Accepted Article

Title: Carbon Dioxide Conversion Upgraded by Host-Guest Cooperation between Nitrogen-rich Covalent Organic Framework and Imidazolium-based Ionic Polymer

Authors: Hong Zhong, Jinwei Gao, Rongjian Sa, Shuailong Yang, Zhicheng Wu, and Ruihu Wang

To be cited as: *ChemSusChem* 10.1002/cssc.202001658

Link to VoR: https://doi.org/10.1002/cssc.202001658

WILEY-VCH

Carbon Dioxide Conversion Upgraded by Host-Guest Cooperation between Nitrogen-rich Covalent Organic Framework and Imidazolium-based Ionic Polymer

Hong Zhong,[a,b] Jinwei Gao,[b] Rongjian Sa,*[a] Shuailong Yang[b] Zhicheng Wu[b] and Ruihu Wang*[b]

Abstract: The chemical conversion of CO_2 into value-added chemicals is one promising approach for CO_2 utilization. It is crucial to explore highly efficient catalysts containing task-specific components for CO_2 fixation. Here, we reported a host-guest catalytic system by integrating nitrogen-rich covalent organic framework (TT-COF) and imidazolium-based ionic polymer (ImIP), which serve as hydrogen bonding donor and nucleophilic agent, respectively, for cooperatively facilitating the activation of the epoxides and subsequent CO_2 cycloaddition. The catalytic activity of the host-guest system is remarkably superior to those of ImIP, TT-COF and their physical mixture. Furthermore, selective adsorption for CO_2 over N_2 renders this catalytic system to be effective for the cycloaddition reaction of the simulated flue gas. The protocols for the unification of two catalytically active components provide new opportunities for the development of composite systems in multiple applications.

Introduction

Carbon dioxide (CO_2) is major product in the combustion of fossil fuels, the excessive emission into the atmosphere is regarded as primary causes for global warming and climate change.[1] The capture and chemical conversion of CO_2 into value-added chemicals has captured considerable interests because CO_2 is also a cheap, nontoxic, renewable and readily available carbon source.[2] Among a variety of available catalytic methodologies for chemical fixation of CO_2, the cycloaddition of CO_2 with the epoxides to form cyclic carbonates is one efficient, atom-economic and environment-benign process.[3] The ring opening of the epoxides is considered as the rate-determining step in the catalytic reaction, great efforts have been made to control the activation of the epoxides and subsequent CO_2 reaction with the opened ring.[4] In the context, metal-free heterogeneous catalysts containing hydrogen bonding donors (hydroxyl, amino and carboxyl *et al.*) and nucleophilic groups (halide anion *et al.*) are of utmost importance.[4b,5] They can work in a cooperative activation pathway for CO_2 cycloaddition, but the limited porosities in most of heterogeneous systems are disfavorable for mass transfer and the accessibility of the active sites, which leads to relatively inferior activities.[6] It is desirable to develop new classes of porous catalysts containing dual components for the adsorption and activation of CO_2 as well as subsequent cycloaddition reaction with the epoxides.

Covalent organic frameworks (COFs) are the emerging crystalline porous materials consisting of organic building blocks connected through covalent bonds.[7] Modular synthetic strategy allows CO_2-philic components and nitrogen-rich groups to be homogeneously embedded into the frameworks through judicial selection of versatile synthetic methods, which facilitates CO_2 adsorption and catalytic conversion.[8] A few COFs have been recently employed as metal-free catalysts for the cycloaddition of CO_2 with the epoxides.[9] It has been documented that the grafting of imidazolium-based ionic liquids onto pore wall of COFs remarkably improves catalytic efficiency in the absence of cocatalysts and additives,[10] but tedious synthetic procedures for either ionic liquids-functionalized building blocks or postsynthetic modification processes have been restricted their applications. As a promising alternative method, strong entrap ability of COFs can integrate ionic liquids or their polymers into COFs to form a library of heterogeneous composite materials, the cooperative interactions of dual components could improve catalytic activity of CO_2 cycloaddition reaction.[11] However, metal-free heterogeneous catalysts based on the composites of COFs and ionic polymers have been not reported hitherto.

As a proof-of-concept study, herein, we presented one host-guest catalytic system by integrating nitrogen-rich COF with imidazolium-based ionic polymer (ImIP), these components show the morphology of nanosheets and nanowires, respectively, which are conductive to the availability of catalytically active sites. The resultant host-guest composite exhibits good CO_2 sorption ability, high adsorption selectivity of CO_2 over N_2. The excellent catalytic activity and superior recyclability are achieved in the cycloaddition reaction of CO_2 with the epoxides.

Results and Discussion

The synthetic route of ImIP@TT-COF was shown in Figure 1. The aqueous solution of 1H-1,2,4-triazole-3,5-diamine (TDA) and 4-methylbenzenesulfonic acid was layered on the top of dichloromethane solution of 2,4,6-triformylphloroglucinol (TP), subsequent acid-catalyzed Schiff-based reaction at the interface of solution generated TT-COF. The ultrasonic treatment of as-prepared TT-COF in DMF solution of 3-ethyl-1-vinyl-imidazolium

---

[a] H. Zhong, Prof. R. Sa.
Institute of Oceanography, Fujian Key Laboratory of Functional Marine Sensing Materials, Minjiang University, Fuzhou, Fujian 350108, China
E-mail: rjsa@mju.edu.cn.
[b] H. Zhong, J. Gao, S. Yang, Z. Wu, Prof. R. Wang.
State Key Laboratory of Structural Chemistry
Fujian Institute of Research on the Structure of Matter, Chinese Academy of Sciences
350007, Fuzhou, China
E-mail: ruihu@fjirsm.ac.cn.

Supporting information for this article is given via a link at the end of the document.

bromide, followed by free-radical polymerization in the presence of azobisisobutyronitrile (AIBN) gave rise to ImIP@TT-COF.

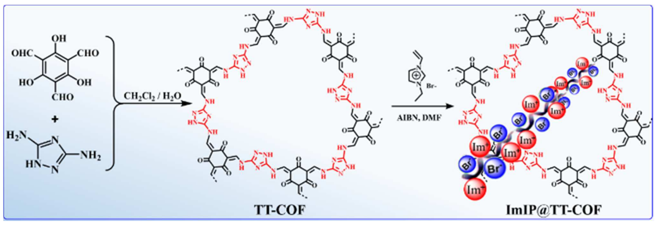

Figure 1. Schematic illustration for the fabrication of ImIP@TT-COF.

The compositions and structures of TT-COF and ImIP@TT-COF were defined by Fourier-transform infrared (FTIR), solid-state ^{13}C NMR spectra and powder X-ray diffraction (PXRD). As shown in Figure 2a, the typical carbonyl peak of TP at 1647 cm^{-1} disappears in the FTIR spectrum of TT-COF, while the C=C and C-N stretching peaks concomitantly occur at 1593 and 1261 cm^{-1}, respectively, revealing successful polymerization and the formation of the β-ketoenamine-linked framework structure.[12] Notably, the FTIR spectrum of ImIP@TT-COF is almost identical with that of TT-COF, indicative of structural preservation of TT-COF after the incorporation of ImIP. In the solid-state ^{13}C NMR spectra, both of them show characteristic signals of carbon atoms of C=O, C-N and β-ketoen C=C bonds (Figure 2b).[12a,13] The peaks of carbon atoms from ImIP are observed at 136, 122, 45, 37, 31 and 14 ppm in ImIP@TT-COF, which validates the integration of ImIP with TT-COF. PXRD pattern shows the diffraction peaks of TT-COF are similar to the reported results,[13a,14] the introduction of ImIP has no obvious effects on the peak positions and intensity (Figure 2c). The elemental analysis of charge-balanced bromide reveals the content of imidazolium group in ImIP@TT-COF is 0.52 mmol g^{-1}.

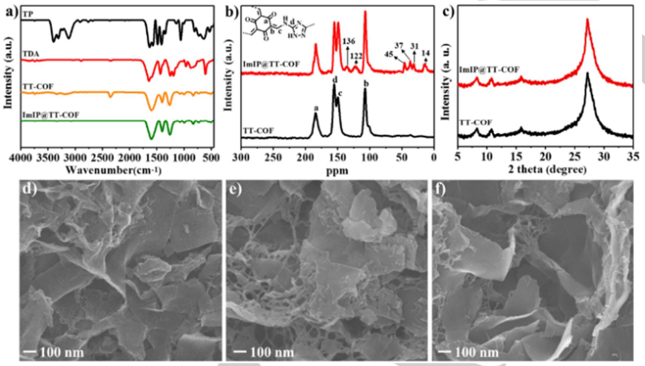

Figure 2. (a) FTIR spectra for TT, TDA TT-COF and ImIP@TT-COF. (b) Solid-state ^{13}C NMR spectra of TT-COF and ImIP@TT-COF. (c) PXRD patterns of TT-COF and ImIP@TT-COF. SEM images for (d) TT-COF, (e) ImIP@TT-COF, and (f) ImIP@TT-COF-6run.

Field-emission scanning electron microscopy (SEM) images show that TT-COF is mainly composed of nanosheets, the nanosheets are known to possess more accessible active sites for the activation of the epoxides than spherical counterpart synthesized by solvothermal approach.[13b,14b] Notably, nanowires corresponding to ImIP can be clearly observed in the surface of TT-COF nanosheets in ImIP@TT-COF (Figure 2d, e). The morphology benefits the nucleophilic attack of Br^- to the activated epoxides by TT-COF. ImIP@TT-COF possesses excellent chemical stability. The PRXD patterns have no obvious variation after immersed in various organic solvents, HCl (1 M) and NaOH (1 M) for 3 days (Figure S2). Thermogravimetric analysis (TGA) curve indicate that TT-COF is stable before 270 °C (Figure S1). The thermal stability of ImIP@TT-COF is slightly lower than that of TT-COF owing to the presence of ImIP.[15]

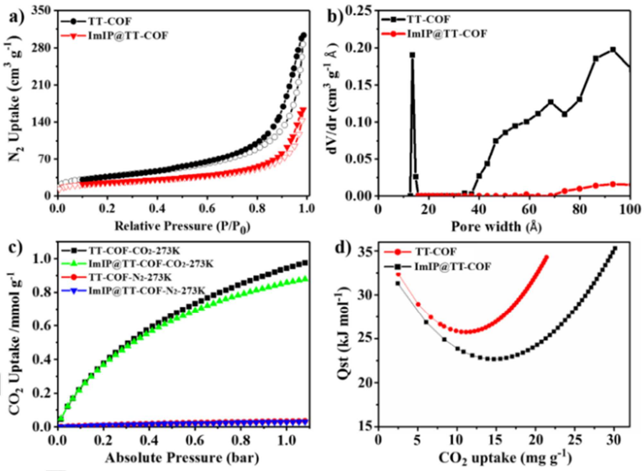

Figure 3. (a) N_2 sorption isotherms of TT-COF and ImIP@TT-COF at 77 K. (b) Pore size distributions for TT-COF and ImIP@TT-COF. (c) CO_2 and N_2 sorption isotherms of TT-COF and ImIP@TT-COF at 273 K. (d) CO_2 Q_{st} for TT-COF and ImIP@TT-COF.

The porosities of TT-COF and ImIP@TT-COF were investigated by nitrogen physisorption at 77 K (Figure 3a). The nitrogen sorption isotherm exhibits type II adsorption branch.[16] The obvious hysteresis and steep rise of nitrogen uptake at high relative pressure suggests the presence of mesopores.[16b,17] Brunauer-Emmett-Teller (BET) specific surface area and total pore volume of TT-COF are 132.3 m^2 g^{-1} and 0.47 cm^3 g^{-1}, respectively, which are decreased in ImIP@TT-COF to 46 m^2 g^{-1} and 0.11 cm^3 g^{-1}, respectively, due to both partial pore filling and mass increment after ImIP introduction.[17b] The pore size distribution reveals that TT-COF possesses micro- and mesopores, which are significantly diminished in ImIP@TT-COF (Figure 3b). CO_2 adsorption properties of TT-COF and ImIP@TT-COF were also investigated. The CO_2 capture amounts for TT-COF at 273 K and 298 K are 0.97 and 0.61 mmol g^{-1}, respectively (Figure 3c, S3). Unexpected, ImIP@TT-COF shows similar CO_2 uptake amounts of 0.88 and 0.52 mmol g^{-1} at 273 K and 298 K, respectively, although its BET specific surface area and total pore volume are much lower than that of TT-COF. The adsorption selectivity of CO_2 over N_2 was further examined. Both TT-COF and ImIP@TT-COF exhibit high CO_2 adsorption selectivity over N_2. The selectivities at 273 K in TT-COF and ImIP@TT-COF are 28.2 and 28.7, respectively (Figure 3c). The preferable adsorption toward CO_2 allows for the application in chemical fixation of post-combustion CO_2.[4b,18] The isosteric heats of adsorption (Q_{st}) for CO_2 were also investigated

(Figure 3d). The initial Q_{st} values for TT-COF and ImIP@TT-COF are 26.3 and 22.5 kJ mol^{-1}, respectively, which suggests CO_2 sorption in TT-COF and ImIP@TT-COF is physisorption (< 40 kJ mol^{-1}) other than chemisorption.[19] Thus, their interactions with CO_2 are suitable for chemical conversion of the adsorbed CO_2 molecules.

Considering high CO_2 adsorption capacity, rich nitrogen content and periodic triazolyl units in TT-COF and ImIP@TT-COF, their catalytic application in the cycloaddition reaction of CO_2 with 2-(chloromethyl)oxirane was first investigated in the absence of solvents, co-catalysts and additives. When the catalytic reaction was conducted under atmospheric CO_2 in the presence of 30 mg catalyst at 120 °C for 10 h, TT-COF and ImIP afforded 4-(chloromethyl)-1,3-dioxolan-2-one in 43% and 36% GC yields, respectively (Figure 4a). However, a quantitative yield was achieved for ImIP@TT-COF under the same conditions. High activity of ImIP@TT-COF mainly originates from cooperative interactions between two catalytic components, namely charge-balanced Br^- anion of ImIP and hydrogen bonds from TT-COF. To substantiate cooperative effects of TT-COF and ImIP, the catalytic reaction was also conducted using physical mixture of TT-COF and ImIP, a 77% GC yield was obtained for the target product. These observations indicate that the integration of task-specifc components is an important factor for the improvement of catalytic activity in the cycloaddition reaction of CO_2 with 2-(chloromethyl)oxirane.

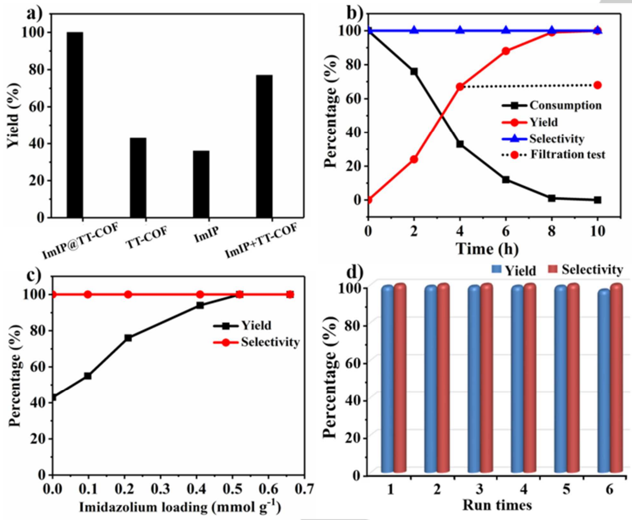

Figure 4. (a) The catalytic activities for ImIP@TT-COF, ImIP, TT-COF and physical mixture of ImIP and TT-COF. (b) The kinetic curves for the cycloaddition reaction. (c) The effect of ImIP loading on the cycloaddition reaction. (d) Recyclability of ImIP@TT-COF in the cycloaddition reaction. Reaction conditions: ImIP@TT-COF (30 mg), 2-(chloromethyl)oxirane (9.2 mmol), CO_2 (1.0 atm) at 120 °C for 10 h.

The kinetic curve of ImIP@TT-COF for the catalytic reaction was shown in Figure 4b. The formation of 4-(chloromethyl)-1,3-dioxolan-2-one and the consumption of 2-(chloromethyl)oxirane gradually increased until the reaction was finished in 8 h. The selectivity of 4-(chloromethyl)-1,3-dioxolan-2-one remains above 99% during the catalytic reaction. Temperature-dependent activity was also examined under atmospheric CO_2 in the temperature range from 25 to 140 °C (Figure S4). Obviously, relatively high temperatures have positive effects on CO_2 cycloaddition. Only trace amount of 2-(chloromethyl)oxirane participated in the reaction at 25 °C, but the GC yields at 80 and 100 °C were increased to 32% and 81%, respectively. The quantitative conversion was achieved at 120 °C. The effects of ImIP loading in ImIP@TT-COF on the catalytic reaction were also explored (Figure 4c). The yield of 4-(chloromethyl)-1,3-dioxolan-2-one gradually enhanced when the loading of ImIP increased to 7.2 wt%, an almost linear relationship between catalytic activity and nucleophilic Br^- anion was observed, revealing strong activation ability of TT-COF toward CO_2 and the epoxides.

The reusability of ImIP@TT-COF was examined using 30 mg of ImIP@TT-COF at 120 °C for 10 h (Figure 4d). After the cycloaddition reaction was conducted at least six times through recharge of CO_2 and 2-(chloromethyl)oxirane, negligible loss of catalytic activity and selectivity were observed. The recovered ImIP@TT-COF after consecutive reaction for six runs (ImIP@TT-COF-6run) was characterized. SEM image (Figure 2f), FTIR (Figure S5) and PRXD pattern (Figure S6) of ImIP@TT-COF-6run have no appreciable change when compared with that of ImIP@TT-COF, suggesting that the excellent durability of ImIP@TT-COF during the catalytic reaction. The filtration test was conducted to examine heterogeneity of ImIP@TT-COF (Figure 4b). After reaction was performed for 4 h, ImIP@TT-COF was quickly filtered off, and the filtrate continued to react for the additional 6 h, negligible change in activity and selectivity confirms that the reaction proceeds in a heterogeneous pathway.

The substrates generality for ImIP@TT-COF was explored using the epoxides containing various groups, such as alkyl halide, alkyl, alkene and ether. As shown in Table 1, a quantitative conversion and 71% GC yield were obtained when 2-(chloromethyl)oxirane (entry 1a) and 2-methyloxirane (entry 2a) were used as substrates, respectively. High activity of 2-(chloromethyl)oxirane is mainly attributed that the electron-withdrawing $-CH_2Cl$ group is favorable for nucleophilic attack of Br^- from ImIP to the epoxide when compared with electron-rich 2-methyloxirane. Notably, a 98% GC yield was achieved for 2-methyloxirane when the reaction time was elongated to 24 h (entry 2b). The use of the epoxides with long alkyl and ether chains, such as 2-butyloxirane, 2-(ethoxymethyl)oxirane and 2-((allyloxy)methyl)oxirane, also afforded the resultant cyclic carbonates in good catalytic activity and selectivity (entries 3a, 3b, 4a, 5a, 6a). As expected, 2-phenyloxirane bearing large steric hindrance gave rise to the target product in low conversion of 66% (entry 7a), while complete cycloaddition to cyclic carbonate was realized when reaction time was enhanced to 48 h (entry 7b). However, the use of the internal cyclohexene oxide gave 31% GC yield in 48h (entry 8a), its lower activity than those of terminal epoxides is consistent with previous reports.[10a, 20] It is noteworthy that the reaction of diepoxide with CO_2 generated the target product in a 94% GC yield after 48 h (entry 9a).

Given high activity and preferable adsorption of CO_2 over N_2, the application of this catalytic system for transformation of post-combustion CO_2 was further evaluated (Table 1). A mixed gas containing 0.15 atm CO_2 and 0.85 atm N_2 was used to simulate flue gas from the power plant. ImIP@TT-COF exhibited high catalytic activity for the cycloaddition reaction of 2-(chloromethyl)oxirane with the simulated flue gas, and 100 % conversion was obtained in the presence of 30 mg catalyt at 120 °C for 24 h (entry 1b). The use of 2-methyloxirane gave rise to the resultant product in a 55% GC yield (entry 2c), which was increased to 85% for reaction time of 48 h (entry 2d). Interestingly, the epoxides with long alkyl carbon chain showed lower conversion than that of the epoxides with long ether chain (entries 3c, 4b, 5b, 6b). ImIP@TT-COF is also effective for 2-phenyloxirane with bulkier steric hindrance and the internal cyclohexene oxide, the target products were obtained in 66 and 17% GC yields in 48 h, respectively (entries 7c, 8b). Notably, when diepoxide was used as substrate, the resultant product was obtained in 51% conversion and 100% selectivity (entry 9b).

Table R1. The cycloaddition reaction of CO_2 with the epoxides catalyzed by ImIP@TT-COF[a]

Entry	Epoxide	Product	P_{CO2} (atm)	Time (h)	Yield[b] (%)	Select.[b] (%)
1a	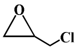	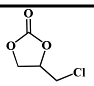	1	10	>99	99
1b			0.15	24	>99	99
2a		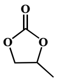	1	10	71	>99
2b			1	24	98	>99
2c			0.15	24	55	>99
2d			0.15	48	85	>99
3a	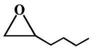	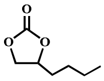	1	24	63	>99
3b			1	48	96	>99
3c			0.15	48	53	>99
4a	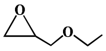	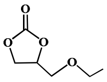	1	24	>99	>99
4b			0.15	48	86	>99
5a	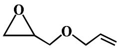	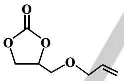	1	24	>99	>99
5b			0.15	48	89	>99
6a	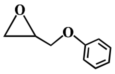	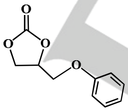	1	24	96	>99
6b			0.15	48	83	>99
7a	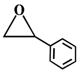	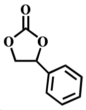	1	24	66	>99
7b			1	48	>99	>99
7c			0.15	48	66	>99
8a	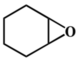	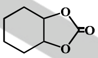	1	48	31	>99
8b			0.15	48	17	>99
9a	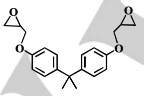	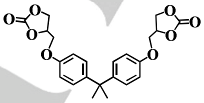	1	48	94	>99
9b			0.15	48	51	>99

[a] Reaction conditions: 2-(chloromethyl)oxirane (9.2 mmol), ImIP@TT-COF (30 mg), 120 °C, [b]GC yield.

To get fundamental insight into cooperative roles of TT-COF and ImIP in the cycloaddition reaction, the density functional theory (DFT) calculations were carried out using Gaussian 09 package.[21] There are two types of interactions between the model molecule of TT-COF and 2-(chloromethyl)oxirane. One is that the lone pair of electrons in the 4-positioned triazolyl nitrogen atom of the model molecule interact with the *β*-carbon atom of the 2-(chloromethyl)oxirane, hydrogen bonds between hydrogen atom of the adjacent N-H groups and the oxygen atom of 2-(chloromethyl)oxirane are simultaneously formed (Figure 5a). The dual interactions increase the C-O bond distance in the *β*-carbon atom of 2-(chloromethyl)oxirane from 1.439 to 1.442 Å. The energy for the interactions is 18.04 kJ mol^{-1}. CO_2 is also activated by the model molecule, giving rise to the bond angle of

178.8° and the interaction energy of 15.36 kJ mol^{-1}. The other is that the 2-positioned nitrogen atom and 1-positioned hydrogen atom in the triazolyl units interact with 2-(chloromethyl)oxirane (Figure 5b), the corresponding C-O bond distance and the interaction energy are further increased to 1.456 Å and 34.45 kJ mol^{-1}, respectively, which are more conducive to the ring opening of the epoxides. In addition, the increment for both bond angle variation of linear CO_2 and the interaction energy between CO_2 and the model molecule are also observed. These results clearly indicate that 2-(chloromethyl)oxirane are preferable for being activated by triazolyl moieties of TT-COF.

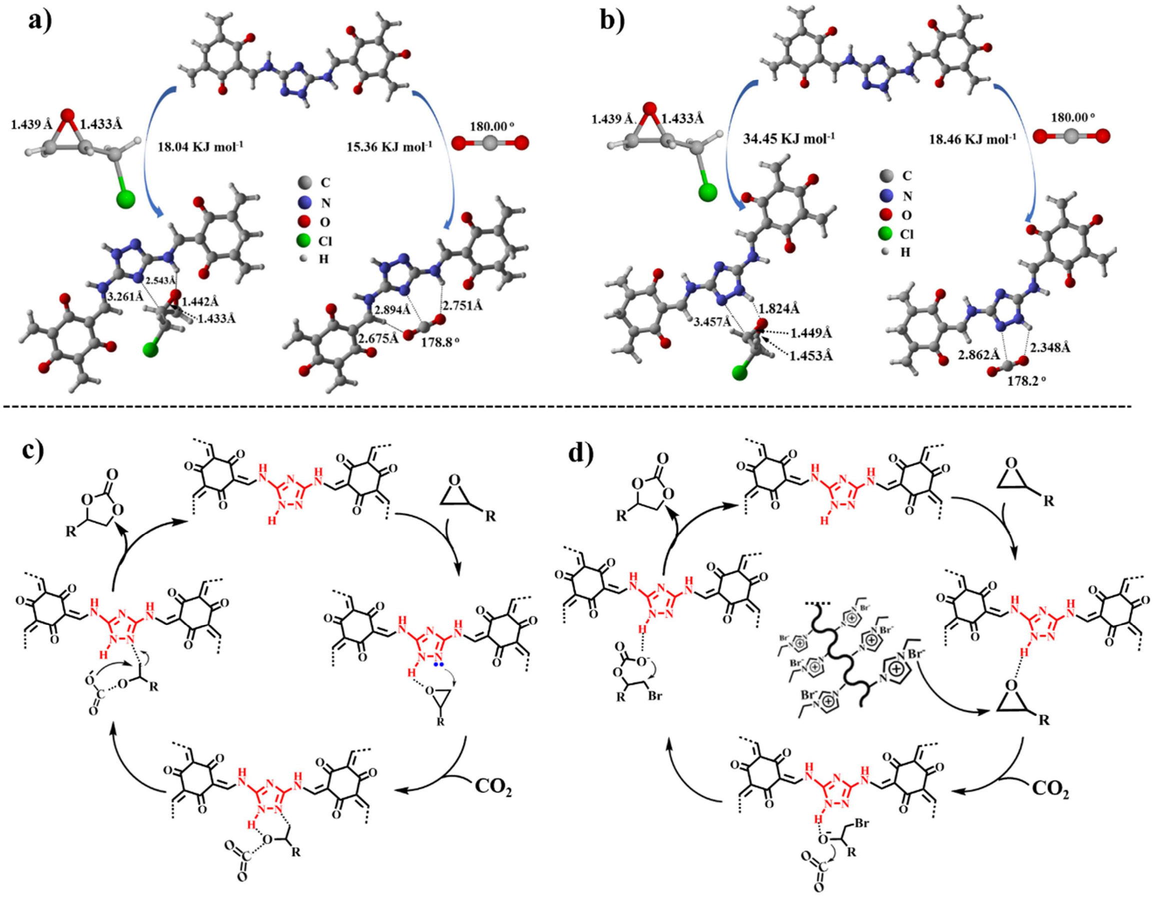

Figure 5. (a,b) The calculated interactions for the model molecule of TT-COF with 2-(chloromethyl)oxirane and CO_2. The proposed mechanisms for the cycloaddition reaction catalyzed by (c) TT-COF and (d) ImIP@TT-COF.

The plausible mechanism for the cycloaddition reaction has been proposed.[18a,22] For TT-COF, N-H groups of triazolyl units in TT-COF can activate C-O bond of the epoxides through hydrogen bonding interactions (Figure 5c).[5e,23] Meanwhile, the aromatic nitrogen atom of triazolyl units interacts with the *β*-carbon atom of the epoxide through lone pair of electrons,[24] resulting in the ring-opening of the epoxides, subsequent coupling with CO_2 forms the cyclic carbonates with synchronous recovery of TT-COF, but the acticity is low owing to weak necleophicity of aromatic nitrogen atoms when compared with that of halide anions. When ImIP is introduced into TT-COF, the flexibility and movability of the nucleophilic Br$^-$ anion from ImIP render task-specific components in ImIP@TT-COF efficiently synergistic interaction (Figure 5d),[11a,25] and leading to the increment of catalytic activity. The ring-opened oxyanion intermediate is stabilized by hydrogen bonds with N-H groups. Simultaneously, the interaction of the oxyanion intermediate with CO_2 generates the alkyl carbonate species. The intramolecular ring closure with the release of bromide anion gives rise to the resultant cyclic carbonates and the recovered ImIP@TT-COF.

Conclusions

The concerted heterogeneous catalytic system has been demonstrated through integrating nitrogen-rich TT-COF host and ImIP guest. ImIP@TT-COF possesses good CO_2 sorption ability, high adsorption selectivity of CO_2 over N_2, rich nitrogen contents and periodic hydrogen bonding donor, leading to high concentration of CO_2 around active sites. The nucleophilic Br$^-$ anion from ImIP and hydrogen bonding donor from TT-COF synchronously promote the ring opening of the epoxides for the formation of the oxyanion intermediate. Meantime, the morphology of nanosheets and nanowires are conducive to the availability of catalytically active sites. These advantages enable catalytic activity of ImIP@TT-COF to be much higher than those of individual counterparts and their physical mixture. Moreover, ImIP@TT-COF is also effective for chemical fixation of post-combustion CO_2. This work provides a new protocol for the development of metal-free catalytic systems for chemical conversion of CO_2 into value-added chemicals and other catalytic applications.

Experimental Section

Synthesis of TT-COF: 1,3,5-Triformylphloroglucinol (21.0 mg, 0.1 mmol) in 150 mL of dichloromethane was poured into the beaker, then 50 mL aqueous solution of 1H-1,2,4-triazole-3,5-diamine (14.9 mg, 0.15 mmol) and 4-methylbenzenesulfonic acid (3.44 g, 20 mmol) was carefully added on top of 1,3,5-triformylphloroglucinol solution and a spacer layer was achieved. The system was kept at room temperature for seven days. The resultant yellow power at the interface was isolated by filtration and then successively washed with water, ethanol and dichloromethane. The collected sample was further treated through Soxhlet extraction with dichloromethane for 24 h, and dried under vacuum at 80 ^{o}C to afford TT-COF.

Synthesis of ImIP@TT-COF: The mixture of TT-COF (100 mg) and 3-ethyl-1-vinyl-imidazole bromide (100.0 mg) in dried DMF (10.0 mL) was ultrasonicated for 30 min, and then azobis(isobutyronitrile) (20.0 mg) was added under N_2 atmosphere. After heated at 80 °C for 3 days, the resultant solid was isolated by filtration, successively washed with DMF, acetone and dichloromethane, and then dried under vacuum at 80 ^{o}C to afford ImIP@TT-COF.

Acknowledgements

This work was financially supported by the National Natural Science Foundation of China (21603228, 21673241 and 21975259) and Natural Science Foundation of Fujian Province (2019J01128), Strategic Priority Research Program of the Chinese Academy of Sciences (XDB20000000).

Keywords: Covalent organic framework • Ionic polymer • Imidazolium • Functional motif • Carbon dioxide.

[1] a) M. Pera-Titus, *Chem. Rev.* **2014**, *114*, 1413-1492; b) Q. W. Song, Z. H. Zhou, L. N. He, *Green Chem.* **2017**, *19*, 3707-3728; c) Y. Zhou, W. Zhang, L. Ma, Y. Zhou, J. Wang, *ACS Sustainable Chem. Eng.* **2019**, *7*, 9387-9398; d) J. Li, Y. Han, T. Ji, N. Wu, H. Lin, J. Jiang, J. Zhu, *Ind. Eng. Chem. Res.* **2020**, *59*, 676-684.

[2] a) A. Goeppert, M. Czaun, J. P. Jones, G. K. S. Prakash, G. A. Olah, *Chem. Soc. Rev.* **2014**, *43*, 7995-8048; b) G. Ji, Z. Yang, H. Zhang, Y. Zhao, B. Yu, Z. Ma, Z. Liu, *Angew. Chem. Int. Ed.* **2016**, *55*, 9685-9689; c) D. O. Meléndez, A. Lara-Sánchez, J. Martínez, X. Wu, A. Otero, J. A. Castro-Osma, M. North, R. S. Rojas, *ChemCatChem* **2018**, *10*, 2271-2277; d) R. Luo, X. Liu, M. Chen, B. Liu, Y. Fang, *ChemSusChem* **2020**, DOI: 10.1002/cssc.202001079.

[3] a) S. Wang, C. Xi, *Chem. Soc. Rev.* **2019**, *48*, 382-404; b) X. Sun, L. Lu, Q. Zhu, C. Wu, D. Yang, C. Chen, B. Han, *Angew. Chem. Int. Ed.* **2018**, *57*, 2427-2431; c) J. Qiu, Y. Zhao, Z. Li, H. Wang, M. Fan, J. Wang, *ChemSusChem* **2017**, *10*, 1120-1127; d) F. D. Bobbink, W. Zhong, Z. Fei, P. J. Dyson, *ChemSusChem* **2017**, *10*, 2728-2735.

[4] a) Y. J. Chen, R. C. Luo, Q. H. Xu, J. Jiang, X. T. Zhou, H. B. Ji, *ACS Sustain. Chem. Eng.* **2018**, *6*, 1074-1082; b) R. Gomes, P. Bhanja, A. Bhaumik, *Chem. Commun.* **2015**, *51*, 10050-10053; c) Y. Wang, J. Nie, C. Lu, F. Wang, C. Ma, Z. Chen, G. Yang, *Micropor. Mesopor. Mater.* **2020**, *292*, 109751; d) Y. Zhang, G. Chen, L. Wu, K. Liu, H. Zhong, Z. Long, M. Tong, Z. Yang, S. Dai, *Chem. Commun.* **2020**, *56*, 3309-3312.

[5] a) Z. Guo, Q. Jiang, Y. Shi, J. Li, X. Yang, W. Hou, Y. Zhou, J. Wang, *ACS Catal.* **2017**, *7*, 6770-6780; b) R. C. Luo, Y. J. Chen, Q. He, X. W. Lin, Q. H. Xu, X. H. He, W. Y. Zhang, X. T. Zhou, H. B. Ji, *ChemSusChem* **2017**, *10*, 1526-1533; c) Y. J. Chen, R. C. Luo, Q. H. Xu, J. Jiang, X. T. Zhou, H. B. Ji, *ChemSusChem* **2017**, *10*, 2534-2541; d) M. A. Ziaee,Y. Tang, H. Zhong, D. Tian, R. Wang, *ACS Sustainable Chem. Eng.* **2019**, *7*, 2380-2387.

[6] a) P. Goodrich, H. Q. N. Gunaratne, J. Jacquemin, L. Jin, Y. Lei, K. R. Seddon, *ACS Sustainable Chem. Eng.* **2017**, *5*, 5635-5641; b) B. Aguila, Q. Sun, X. Wang, E. O. Rourke, A. M. Al-Enizi, A. Nafady, S. Ma, *Angew. Chem. Int. Ed.* **2018**, *57*, 10107-10111; c) F. Yuan, J. Tan, J. Guo, *Sci China Chem.* **2018**, *61*, 143-152; d) X. Li, L. Ma, Y. Liu, L. Hou, Y. Wang, Z. Zhu, *ACS Appl. Mater. Interfaces* **2018**, *10*, 10965-10973.

[7] a) H. Li, Q. Pan, Y. Ma, X. Guan, M. Xue, Q. Fang, Y. Yan, V. Valtchev, S. Qiu, *J. Am. Chem. Soc.* **2016**, *138*, 14783-14788; b) D. Jiang, X. Chen, K. Geng, R. Liu, K. T. Tan, Y. Gong, Z. Li, S. Tao, Q. Jiang, *Angew. Chem. Int. Ed.* **2019**, *59*, 5050-5091; c) Q. Liao, W. Xu, X. Huang, C. Ke, Q. Zhang, K. Xi, J. Xie. *Sci. China Chem.* **2020**, *63*, 707-715; d) H. Zhong, R. Sa, H. Lv, S. Yang, D. Yuan, X. Wang, R. Wang, *Adv. Funct. Mater.* **2020**, *30*, 2002654.

[8] a) J. Roeser, K. Kailasam, A. Thomas, *ChemSusChem* **2012**, *5*, 1793-1799; b) W. Yu, S. Gu, Y. Fu, S. Xiong, C. Pan, Y. Liu, G. Yu, *J. Catal.* **2018**, *362*, 1-9; c) V. Saptal, D. B. Shinde, R. Banerjee, B. M. Bhanage, *Catal. Sci. Technol.* **2016**, *6*, 6152-6158; d) Y. Zhi, P. Shao, X. Feng, H. Xia, Y. Zhang, Z. Shi, Y. Mu, X. Liu, *J. Mater. Chem. A* **2018**, *6*, 374-382.

[9] a) J. Qiu, Y. Zhao, Z. Li, H. Wang, Y. Shi, J. Wang, *ChemSusChem* **2019**, *12*, 2421-2427; b) L. G. Ding, B. J. Yao, F. Li, S. C. Shi, N. Huang, H. B. Yin, Q. Guan, Y. B. Dong, *J. Mater. Chem. A* **2019**, *7*, 4689-4698; c) Y. Zhang, H. Hu, J. Ju, Q. Yan, V. Arumugam, X. Jing, H. Cai, Y. Gao, *Chin. J. Catal.* **2020**, *41*, 485-493.

[10] a) S. Jayakumar, H. Li, Y. Zhao, J. Chen, Q. Yang, *Chem. Asian J.* **2017**, *12*, 577-585; b) W. Zhang, F. Ma, L. Ma, Y. Zhou, J. Wang, *ChemSusChem* **2020**, *13*, 341-350; c) M. Buaki-Sogo, H. Garciab, C. Aprile, *Catal. Sci. Technol.* **2015**, *5*, 1222-1230.

[11] a) Q. Sun, B. Aguila, J. Perman, N. Nguyen, S. Ma, *J. Am. Chem. Soc.* **2016**, *138*, 15790-15796; b) C Calabrese, L. F. Liotta, E. Carbonell, F. Giacalone, M. Gruttadauria, C. Aprile, *ChemSusChem* **2017**, *10*, 1202-1209.

[12] a) S. Kandambeth, A. Mallick, B. Lukose, M. V. Mane, T. Heine, R. Banerjee, *J. Am. Chem. Soc.* **2012**, *134*, 19524-19527; b) P. Pachfule, A. Acharjya, J. Roeser, T. Langenhahn, M. Schwarze, R. Schomäcker, A. Thomas, J. Schmidt, *J. Am. Chem. Soc.* **2018**, *140*, 1423-1427.

[13] a) S. Haldar, K. Roy, S. Nandi, D. Chakraborty, D. Puthusseri, Y. Gawli, S. Ogale, R. Vaidhyanathan. *Adv. Energy Mater.* **2018**, *8*, 1702170; b) C. Liu, Y. Jiang, A. Nalaparaju, J. Jiang, A. Huang, *J. Mater. Chem. A* **2019**, *7*, 24205-24210.

[14] a) S. Mitra, S. Kandambeth, B. P. Biswal, A. Khayum, C. K. Choudhury, M. Mehta, G. Kaur, S. Banerjee, A. Prabhune, S. Verma, S. Roy, U. K. Kharul, R. Banerjee. *J. Am. Chem. Soc.* **2016**, *138*, 2823-2828; b) W. Liu, X. Li, C. Wang, H. Pan, W. Liu, K. Wang, Q. Zeng, R. Wang, J. Jiang, *J. Am. Chem. Soc.* **2019**, *141*, 17431-17440.

[15] a) H. Zhong, Y. Wang, C. Cui, F. Zhou, S. Hu, R. Wang, *Chem. Sci.* **2018**, *9*, 8703-8710; b) Z. Li, Z. Xiao, S. Wang, Z. Cheng, P. Li, R. Wang, *Adv. Funct. Mater.* **2019**, *29*, 1902322.

[16] a) M. D. Donohue, G. L. Aranovich, *Adv. Colloid Interface Sci.* **1998**, *76-77*, 137-152; b) H. Zhong, C. Liu, Y. Wang, R. Wang, M. Hong, *Chem.*

Sci. **2016**, *7*, 2188-2194.

[17] a) X. Wang, Y. Zhou, Z. Guo, G. Chen, J. Li, Y. Shi, Y. Liu, J. Wang, *Chem. Sci.* **2015**, *6*, 6916-6924; b) Y. Chen, R. Luo, J. Bao, Q. Xu, J. Jiang, X. Zhou, H. Ji, *J. Mater. Chem. A* **2018**, *6*, 9172-9182. c) H. Zhong, C. Yang, L. Fan, Z. Fu, X. Yang, X. Wang, R. Wang, *Energy Environ. Sci.* **2019**, *12*, 418-426.

[18] a) C. Cui, R. Sa, Z. Hong, H. Zhong, R. Wang, *ChemSusChem* **2020**, *13*, 180-187; b) H. Zhong, Y. Su, X. Chen, X. Li, R. Wang, *ChemSusChem* **2017**, *10*, 4855-4863; c) H. Song, Y. Wang, M. Xiao, L. Liu, Y. Liu, X. Liu, H. Gai, *ACS Sustain. Chem. Eng.* **2019**, *7*, 9489-9497.

[19] a) e) T. T. Liu, R. Xu, J. D. Yi, J. Liang, X. S. Wang, P. C. Shi, Y. B. Huang, R. Cao, *ChemCatChem* **2018**, *10*, 2036-2040; b) H. Zhong, Z. Hong, C. Yang, L. Li, Y. Xu, X. Wang, R. Wang, *ChemSusChem* **2019**, *12*, 4493-4499.

[20] a) W. L. Dai, B. Jin, S. L. Luo, X. B. Luo, X. M. Tu, C. T. Au, *Catal. Sci. Technol.* **2014**, *4*, 556-562; b) M. Liu, K. Gao, L. Liang, J. Sun, L. Sheng, M. Arai, *Catal. Sci. Technol.* **2016**, *6*, 6406-6416.

[21] a) M. J. T. Frisch, G. W. H. B. Schlegel, *et al, Gaussian 09, Revision E.01*; Gaussian, Inc.: Wallingford CT, **2010**; b) J. Gao, L. Li, C. Cui, M. A. Ziaee, Y. Gong, R. Sa, H. Zhong, *RSC Adv.* **2019**, *9*, 13122-13127.

[22] a) M. Liu, L. Liang, X. Li, X. Gao, J. Sun, *Green Chem.* **2016**, *18*, 2851-2863; b) W. L. Dai, L. Chen, S. F. Yin, S. L. Luo, C. T. Au, *Catal. Lett.* **2010**, *135*, 295-304; c) W. G. Cheng, X. Chen, J. Sun, J. Q. Wang, S. J. Zhang, *Catal. Today* **2013**, *200*, 117-124; d) X. Meng, H. He, Y. Nie, X. Zhang, S. Zhang, J. Wang, *ACS Sustainable Chem. Eng.* **2017**, *5*, 3081-3086.

[23] a) X. L. Meng, Y. Nie, J. Sun,W. G. Cheng, J. Q. Wang, H. Y. He, S. J. Zhang, *Green Chem.* **2014**, *16*, 2771-2778; b) M. H. Anthofer, M. E. Wilhelm, M. Cokoja, M. Drees, F. E. Kühn, *ChemCatChem* **2015**, *7*, 94-98; c) C. Yue, D. Su, X. Zhang, W. Wu, L. Xiao, *Catal. Lett.* **2014**, *144*, 1313-1321

[24] S. Subramanian, J. Park, J. Byun, Y. Jung, C. T. Yavuz, *ACS Appl. Mater. Interfaces* **2018**, *10*, 9478-9484.

[25] Z. Zhang, F. Fan, H. Xing, Q. Yang, Z. Bao, Q. Ren, *ACS Sustainable Chem. Eng.* **2017**, *5*, 2841-2846.

Entry for the Table of Contents

FULL PAPER

The host-gust composites have been developed through integrating nitrogen-rich covalent organic framework and imidazolium-based ionic polymer, they serve as hydrogen bonding donor and nucleophilic agent, respectively, for the activation and ring opening of the epoxides. The excellent catalytic activity and recyclability are achieved in the cycloaddition reaction of CO_2 with epoxides.

Hong Zhong, Jinwei Gao, Rongjian Sa, Shuailong Yang, Zhicheng Wu and Ruihu Wang**

Page No. – Page No.

Carbon Dioxide Conversion Upgraded by Host-Guest Cooperation between Nitrogen-rich Covalent Organic Framework and Imidazolium-based Ionic Polymer